Journal of Hazardous Materials 176 (2010) 174–180

Contents lists available at ScienceDirect

Journal of Hazardous Materials

journal homepage: www.elsevier.com/locate/jhazmat

Research article

Arsenate removal from aqueous solution using synthetic siderite

Huaming Guo*, Yuan Li, Kai Zhao

School of Water Resources and Environment, China University of Geosciences, Beijing 100083, China

ARTICLE INFO

Article history:
Received 5 September 2009
Received in revised form 30 October 2009
Accepted 1 November 2009
Available online 10 November 2009

Keywords:
Adsorption
Arsenic(V)
Iron hydroxides
Kinetic
Thermodynamic

ABSTRACT

The study was carried out to evaluate the feasibility of synthetic siderite for As(V) removal from aqueous solution. Batch experiments were performed to investigate effects of various experimental parameters such as contact time (10 min–8 h), initial As(V) concentration (0.5–60.0 mg/L), temperature (15, 25, 35 and 45 °C), pH (2.0–10.0) and the presence of competing anions on As(V) adsorption on the synthetic siderite. Kinetic data reveal that the uptake rate of As(V) was rapid at the beginning and 90% adsorption was completed within 10 min at 45 °C and equilibrium was achieved within 3 h. The adsorption process was well described by pseudo-second-order kinetics model. The adsorption data better fitted Langmuir isotherm at low temperatures (i.e., 15 and 25 °C), while Freundlich isotherm at relatively high temperatures (35–45 °C). The maximum adsorption capacity calculated from Langmuir isotherm model was up to 31 mg/g. Thermodynamic study indicates an exothermic nature of adsorption and a spontaneous and favorable process. The optimum pH for As(V) removal was broad, ranging from 3.0 to 10.0. The As(V) adsorption was impeded by the presence of SiO_3^{2-}, followed by PO_4^{3-} and NO_3^-. The adsorption process appeared to be controlled by the chemical process. The high As uptake may attribute to both coprecipitation of As with goethite and lepidocrocite forming during the reaction and subsequent adsorption of As on these minerals.

1. Introduction

High As groundwaters have been found in many countries, including Bangladesh, West Bengal, Argentina, China, Mexico, the United States, Chile and Japan [1,2]. Many high-As groundwaters have been used for drinking water. Long-term exposure to As in drinking water has caused a variety of chronic health problems, including skin diseases (pigmentation, dermal hyperkeratosis, skin cancer), cardiovascular, neurological, hematological, renal and respiratory diseases, as well as lung, bladder, liver, kidney and prostate cancers [3]. In order to protect public health, the World Health Organization has set a provisional guideline limit of 10 μg/L for As in drinking water [4], which was subsequently adopted by the European Union [5] and the United States [6]. The lowering of As drinking water standard requires effective and cheap technologies for As removal from the As drinking water.

Among a variety of technologies (including precipitation-coagulation, membrane separation, ion exchange, lime softening and adsorption), adsorption and coagulation are believed to be the cheapest As removal methods. Although coagulation with iron and aluminium salts is more effective, the requirement of skilled operator and the introduction of contaminants into the water limit its application in small community and household levels. Since solid adsorbents are easy to handle and are appropriate for use in country side where high As groundwater mostly occurs, adsorption has received much attention on As removal. Iron containing substances have been widely investigated to remove As from aqueous solution due to their high specific surface area, including Mn-substituted Fe oxyhydroxide [7], granular ferric hydroxide [8] ferrihydrite [9], goethite [10], zero valent iron [11], Ce(IV)-doped Fe oxide [12], natural hematite and natural siderite [13]. Although natural siderite has been found to be a potential adsorbent for As removal, the kinetic rates for As adsorption are relatively low [2,13]. In comparison with the natural siderite having been aged for a long-term period, synthetic siderite has much more active sites on the surface. However, a review of the literature shows that little has been done to evaluate the applicability of synthetic siderite for remediation of As from high As drinking water.

This study investigates the feasibility of the synthetic siderite for As(V) removal from aqueous solution. The main objectives are (i) to understand the As(V) adsorption kinetics, (ii) to evaluate the impact of temperature, pH and coexisting anions on the As(V) removal kinetics and/or capacities; and (iii) to describe and explain some important thermodynamic parameters.

* Corresponding author. Tel.: +86 10 8232 1366; fax: +86 10 8232 1081.
E-mail address: hm.guo@hotmail.com (H. Guo).

0304-3894/$ – see front matter © 2009 Elsevier B.V. All rights reserved.
doi:10.1016/j.jhazmat.2009.11.009

2. Materials and methods

2.1. Materials

All reagents used in this study, including ferrous sulfate ($FeSO_4{\cdot}7H_2O$) and ammonium hydrocarbonate (NH_4HCO_3), were of analytical grade. Stock As(V) solution (1000 mg/L) were prepared from sodium hydrogen arsenate ($Na_2HAsO_4{\cdot}7H_2O$, Fluka Chemical) using deionized water. All glasswares and sample bottles were rinsed with 10% HNO_3 for at least 24 h, soaked with tap water, and finally rinsed with deionized water three times.

Artificial siderite was synthesized with ferrous sulfate ($FeSO_4{\cdot}7H_2O$) and ammonium bicarbonate (NH_4HCO_3). Ferrous carbonate was precipitated by mixing 1 M Fe^{2+} with 2 M HCO_3^- at room temperature. The precipitate was filtered with 0.45 μm membrane. After rinsed with deionized water for three times, the artificial siderite was air-dried for 24 h and ground to powder (200 mesh). The product was then kept in a desiccator.

2.2. Batch experiments

The batch experiments to study the removal of As from solution were carried out by reacting 50 mL of As solution in 100 mL polyethylene bottles with 0.10 g of the adsorbent. The bottles were immersed in a shaking water bath at predetermined temperature (15, 25, 35, 45 °C). The shaker speed was controlled at 150 rpm. After a predetermined contact time, the aqueous samples in each bottle were decanted and centrifugated at 4500 rpm for 5 min, and then filtered through a 0.45 μm cellulose acetate filter. The supernatant was analyzed for dissolved Fe and total As. Unless specified otherwise, the concentration of the As species was expressed as the element (As).

The effect of contact time (10 min–8 h) was examined at 25 and 45 °C with initial As(V) concentrations of 10.0 mg/L. Adsorption isotherm studies were conducted by varying initial As(V) concentrations (0.5–60.0 mg/L) at different temperatures (i.e., 15, 25, 35, and 45 °C). The effect of solution pH was investigated by adjusting solution pH from 2.0 to 10.0 using 0.05 M HCl and 0.01 M NaOH solutions with an initial As(V) concentration of 1.0 mg/L. To determine the effect of other competitive anions on As adsorption, batch tests were performed using solutions of 1.0 mg/L As(V) containing 0.5, 1, 2, 5,10 and 20 mg/L of P (as PO_4^{3-}), N (as NO_3^-), S (as SO_4^{2-}) or Si (as SiO_3^{2-}), separately. After a 3 h reaction time, the suspension was filtered through a 0.45 μm cellulose acetate filter and analyzed for total As, as described above.

2.3. Analytical methods

Solution pH was monitored by a standard pH meter (Sartorius, PB-10). Dissolved Fe and As was analyzed by ICP-MS (7500C, Agilent). The mineral composition of the adsorbents was determined by X-ray diffraction analysis (XRD), using a URD-6 powder diffractometer (Co Kα radiation, graphite monochromator, 2θ range 2.6–70°, step 0.01°, counting time 5 s per step). Morphological analysis of the pristine and used adsorbent was performed by scanning electron microscopy (SEM) using Zeiss SUPRA 55 microscope (at 15 kV) with energy-dispersive X-ray analyses.

3. Results and discussion

3.1. Effect of contact time

The As(V) adsorption kinetic study was carried out with adsorbent dosage of 2 g/L and initial As concentration of 10.0 mg/L at 25 and 45 °C, respectively. Results are shown in Fig. 1. It demonstrates that adsorbed As significantly increased with an increase in contact time. The adsorption rate was rapid at the initial stage (10 min–1.0 h) and gradually slowed down afterwards. The slower adsorption was likely due to the decrease in adsorption sites on the surface of the adsorbents [14,15]. About 90% As was removed in 10 min at 45 °C, while only 40% at 25 °C. Arsenic concentration was kept relatively constant at contact times >1.0 h at 45 °C. The adsorption equilibrium was generally achieved within 1.0 h. In comparison, adsorption equilibrium time was a little higher at 25 °C. The kinetic data show that As removal mainly occurred within 3.0 h and there was no significant change in residual As concentrations after this time up to 8.0 h. It means that an equilibrium of As adsorption was roughly attained after 3.0 h at 25 °C, which is much shorter than As(V) adsorption on the natural siderite [2,13]. Adsorption experiments in other batches were conducted with the contact time of 3.0 h. It should be noted that the adsorption capacities calculated from the kinetic experiments do not reflect the actual capacities because the experiments were conducted in the presence of a large excess of surface sites. The actual adsorption capacity can be estimated from isotherm results, which are discussed later.

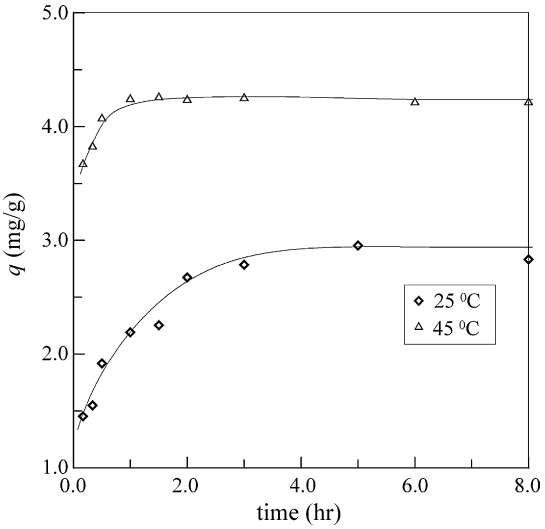

Fig. 1. Effect of contact time on As(V) adsorption on the synthetic siderite (initial As(V) concentration = 10.0 mg/L, adsorbent dosage = 2 g/L).

Results also reveal that the uptake rates of As(V) increased with increasing temperature. Tyrovola et al. observed a similar trend when they used zero-valent iron for the removal of As(V) and As(III) [16]. Other investigators also reported that the As removal rate and the capacity of the adsorbents increased with increasing temperature (e.g., Mn-substituted Fe oxyhydroxide [7], granular ferric hydroxide [8], red mud [17], activated alumina [18]).

3.2. Adsorption kinetic modeling

3.2.1. Pseudo-second-order model

An appropriate kinetic model is often used for quantifying the changes in adsorption with time. Traditionally, the pseudo-first-order Lagergren equation is applied to adsorption kinetics [8,19]. However, a recently introduced pseudo-second-order equation was employed to analyze the kinetic data since it allows evaluating effective adsorption capacity, initial adsorption rate and the rate constant of the kinetic model without any parameters beforehand [20]. The pseudo-second-order Lagergren equation is shown as Eq. (1) [19].

$$\frac{t}{q} = \frac{1}{q_e}t + \frac{1}{K_2 \cdot q_e^2} \quad (1)$$

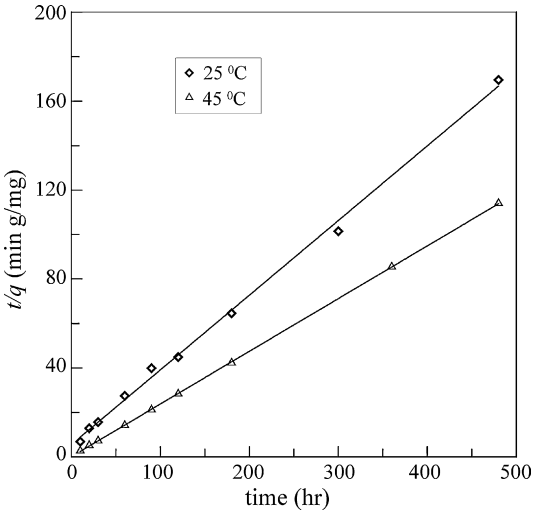

Fig. 2. Plot of Lagergren's pseudo-second-order rate for As(V) adsorption on the synthetic siderite at 25 and 45 °C.

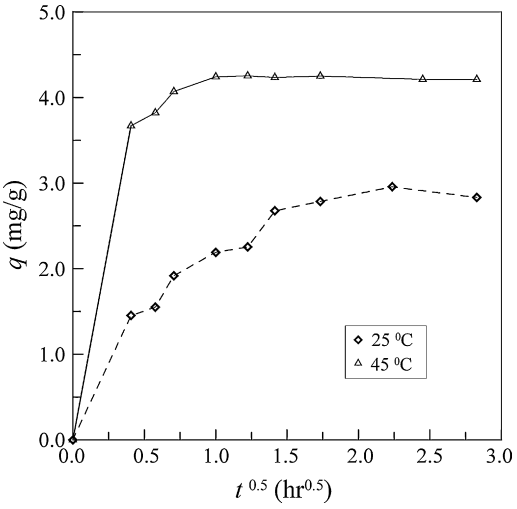

Fig. 3. Intraparticle rate of As(V) adsorption on the synthetic siderite.

where q is the amount of As(V) adsorbed at time t (mg/g), q_e is the amount of As(V) adsorbed at equilibrium (mg/g), K_2 is the equilibrium rate constant of pseudo-second-order adsorption (g/(mg min)).

The plot of t/q versus t (contact time) is shown in Fig. 2. The straight line plots of t/q against t had also been tested to obtain pseudo-second-order rate parameters. The K_2, q_e and correlation coefficients, r^2, values under different conditions were calculated from these plots and are given in Table 1. High correlation coefficients ($r^2 > 0.99$) were observed for all fits, which indicates that the adsorption reaction could be approximated with a pseudo-second-order kinetics model. It suggests that the overall rate of the As(V) adsorption process should be controlled by the chemical process in accordance with the pseudo-second-order reaction mechanism [21].

The initial adsorption rate, h (mg/(g min)), as $t \to 0$, can be defined as:

$$h = K_2 q_e^2 \quad (2)$$

The initial adsorption rate (h) can be calculated based on the pseudo-second-order constants. Results are shown in Table 1. It can be seen that the h value of As(V) adsorption at 45 °C was higher than that at 25 °C.

3.2.2. Webber and Morris model

The use of the intraparticle diffusion model has been greatly explored to analyze nature of the 'rate-controlling step', which is represented by Eq. (3) [22].

$$q = K_{id} t^{0.5} \quad (3)$$

where K_{id} is intraparticle diffusion rate constant (mg/(g min$^{0.5}$)).

According to this model, if adsorption of a solute is controlled by the intraparticle diffusion process, a plot of solute adsorbed against square root of contact time should yield a straight line. The Weber and Morris plots of As(V) adsorption on the synthetic siderite are shown in Fig. 3. Fig. 3 indicates that the intraparticle diffusion was not the only rate-limiting step for the whole reaction. Straight lines with a great correlation coefficient ($r^2 = 0.95$) were obtained in very beginning period (20–30 min), indicating that initial phase may be controlled by the intraparticle diffusion. The greater diffuse rate in the early stage attributed to surface adsorption and gradual adsorption. Afterwards, the intraparticle diffusion began to slow due to the low As concentration in solution [23]. The As was initially adsorbed by the exterior surface of the adsorbent. After the adsorption at the exterior surface reached the saturation, As entered the pores within the particles and was adsorbed by the interior surfaces. The diffusion resistance increased with the increase in the interior adsorption, which led to a decrease in diffusion rate [24]. With the increase in diffusion resistance and the decrease in As concentration in solution, the diffusion processes reached equilibrium. The intraparticle diffusion rate was obtained from the slope of the steep-sloped portion (Table 1). The diffusion rate for As(V) at 45 °C is about two times faster than that at 25 °C, indicating that As was more easily diffused and transported into adsorbent pores at higher temperature.

The equilibrium time for As(V) adsorption on the synthetic siderite was much shorter in comparison with natural siderite with the grain size of 0.125–0.25 mm (i.e., 72 h [13]) and with the grain size of 0.25–0.50 mm (i.e., 24 h [2]). Although there was no information about As(V) adsorption kinetics for natural siderite with grain size 0.07–0.08 mm (about 200 mesh), it seemed that the adsorption equilibrium time was not less than 24 h. It must be noted that adsorption on the synthetic siderite was a relatively quick process predominated by chemical reactions. In contrast, the adsorption on the natural siderite was an essentially more complex process controlled by diffusion, exhibiting the slowest step in the primary and secondary porosity [25].

3.3. Effect of initial As concentration

Effect of initial As concentration on As adsorption were investigated at initial As(V) concentrations between 0.5 and 60.0 mg/L at 15, 25, 35, and 45 °C. The As loadings on the adsorbents (q_e, μg/g)

Table 1
Parameters of pseudo-second-order rate and intraparticle diffusion rate for As(V) adsorption on the synthetic siderite at 25 and 45 °C.

	Lagergren's pseudo-second-order				Intraparticle diffusion rate
	r^2	K_2	q_e (mg/g)	h (mg/(g min))	K_{id} (mg/(g h$^{0.5}$))
25 °C	0.9974	0.0202	2.978	0.179	3.559
45 °C	1.0000	0.4958	4.221	8.834	8.983

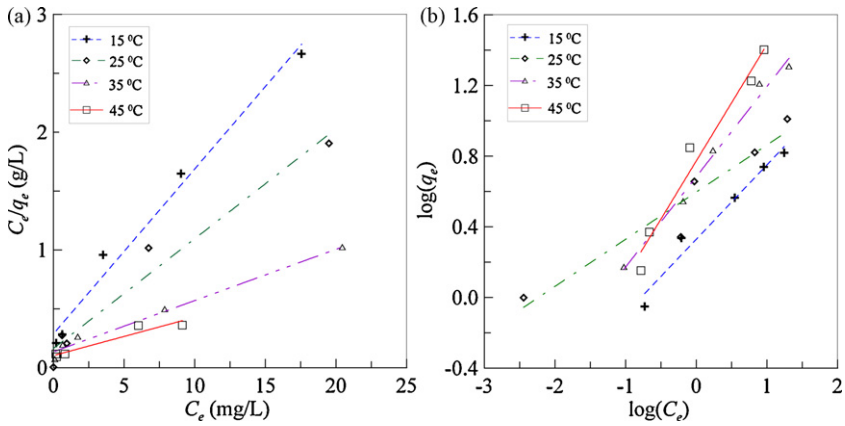

Fig. 4. Isotherms for As(V) adsorption on the synthetic siderite: (a) Langmuir isotherm and (b) Freundlich isotherm.

were calculated from the equilibrium As concentrations (C_e, μg/L) using mass balance. The adsorption loadings varied in the ranges of 0.239–7.57, 0.249–10.25, 0.379–20.14 and 0.370–25.29 mg/g at 15, 25, 35, and 45 °C, respectively. It indicates that As adsorption increased with the increase in reaction temperature.

The adsorption isotherm data (q_e versus C_e) were fitted to Langmuir and Freundlich isotherm models [Eqs. (4) and (5), respectively]. Langmuir isotherm model assumes a monolayer surface coverage limiting the adsorption due to the surface saturation, while Freundlich isotherm model is an empirical model allowing for multilayer adsorption [13].

$$\frac{C_e}{q_e} = \frac{1}{q^0 b} + \frac{C_e}{q^0} \tag{4}$$

$$\log q_e = \log K_F + n \log C_e \tag{5}$$

where C_e is the equilibrium concentration in the solution (mg/L), q_e is the amount adsorbed on the adsorbent at equilibrium (mg/g), q^0 is the maximum adsorption capacity (mg/g), b is a constant related to the adsorption energy (L/mg), K_F is the Freundlich constant denoting the adsorption capacity of the adsorbent [(mg/g)(L/mg)^n], and n is the adsorption intensity parameter. Values of $0.1 < n < 1$ show favorable adsorption of As onto adsorbents [26].

All the adsorption data obtained were fitted to both models as shown in Fig. 4. At 15 and 25 °C, correlation coefficients for Langmuir isotherm model ($r^2 = 0.9735$–0.9868) were a little higher compared to those for Freundlich ($r^2 = 0.9446$–0.9622) (Table 2), while at 35 and 45 °C correlation coefficients for Freundlich isotherm model were higher than those for Langmuir. Therefore, Freundlich isotherm yielded better fit to the experimental data with regard to As adsorption on the synthetic siderite at temperatures of 35 and 45 °C. In contrast, the As(V) adsorption closer followed Langmuir isotherm in comparison with Freundlich isotherm at temperatures of 15 and 25 °C. These facts suggest that As(V) was adsorbed in the form of monolayer coverage on the surface of the adsorbent at low temperatures. Langmuir isotherm model was also used to well describe As(V) adsorption on natural siderite [2], Fe oxide-coated sand [27], granular titanium dioxide adsorbent [28], synthetic goethite [29], and iron-coated sand and manganese-coated sand [30], at 25 °C. Because Freundlich isotherm model can be applied to multilayer sorption as well as non-ideal sorption on heterogeneous surfaces, it could be speculated from our data that the multilayer adsorption would be involved in the process of As removal by the synthetic siderite at relatively higher temperatures (>35 °C).

The values of maximum adsorption capacity (q^0) and Langmuir constant (b) were evaluated from the intercept and slope of the Langmuir plots and given in Table 2. Results show the greatest amount of As was removed at 45 °C, followed by that at 35, 25, and 15 °C. The maximum adsorption, for example, reached 10.73 mg/g at 25 °C. It demonstrates that adsorption capacity increased with an increase in reaction temperature. Although the cost of this material was a little higher than the natural siderite, the adsorption capacity of the synthetic siderite was much greater than the natural siderite. Guo et al. [13] reported that the maximum adsorption capacity of the natural siderite was 0.516 mg/g at 25 °C.

The values of K_F and n were obtained from the slope and intercept of the linear Freundlich plots and listed in Table 2. The K_F indicating the adsorption capacity of the adsorbent increased with the increase in reaction temperature, which is consistent with the results of Langmuir model. The calculated n lies in the range between 0.2 and 0.7, denoting favorable adsorption of As(V) onto the synthetic siderite.

3.4. Thermodynamic study

To evaluate the thermodynamic feasibility and to confirm the nature of the adsorption process, three basic thermodynamic parameters, standard free energy (ΔG^0), standard enthalpy (ΔH^0) and standard entropy (ΔS^0) were calculated using the following equations [Eqs. (6)–(8)].

$$\Delta G^0 = RT \ln\left(\frac{1}{b}\right) \tag{6}$$

$$\ln b = \ln b_0 - \frac{\Delta H^0}{RT} \tag{7}$$

Table 2
Langmuir and Freundlich constants for As(V) adsorption on the synthetic siderite at different temperatures.

Temperature (°C)	Langmuir constants			Freundlich constants		
	q^0 (mg/g)	b (L/mol)	r^2	n	K_F (mg/g)(L/mg)^n	r^2
15	6.86	3.65×10^4	0.9868	0.3668	2.30	0.9622
25	10.73	4.28×10^4	0.9735	0.2960	3.81	0.9446
35	22.99	4.29×10^4	0.9849	0.5109	4.82	0.9932
45	30.77	4.85×10^4	0.9269	0.6503	5.89	0.9845

Table 3
Thermodynamic parameters for As(V) adsorption on the synthetic siderite at different temperatures.

T (°C)	ΔG^0 (kJ/mol)	ΔH^0 (kJ/mol)	ΔS^0 (J/(mol K))
15	−25.23	6.57	110.44
25	−26.51		111.01
35	−27.40		110.30
45	−28.62		110.67

$$\Delta G^0 = \Delta H^0 - T\Delta S^0 \quad (8)$$

where b is Langmuir constant which is related to the energy of adsorption, b_0 is a constant, R is the universal gas constant (8.314 J/(mol K)), and T is the temperature in Kelvin (K).

Calculated values of the energy parameters ΔG^0, ΔH^0 and ΔS^0 are given Table 3. The negative ΔG^0 values indicate the adsorption process was spontaneous. The value of ΔH^0 for As(V) adsorption is 6.57 kJ/mol, suggesting that interaction between As(V) and the synthetic siderite was endothermic in nature. Hence, it can be concluded that the nature of As(V) adsorption was chemical, which is consistent with the results of kinetic study. The decrease in ΔG^0 with the rise in temperature shows an increase in feasibility of adsorption at higher temperatures [31]. The positive ΔS^0 values indicate some structural changes in adsorbate and adsorbent during adsorption reaction [32].

3.5. Effect of solution pH

The solution pH is an important parameter which influences most of the solid/liquid adsorption processes. The adsorption of As(V) on the synthetic siderite was examined at different pH ranging from 2.0 to 10.0 with an initial As(V) concentration of 1.0 mg/L and a contact time of 3.0 h. Results are presented in Fig. 5. It was observed that the As(V) adsorption drastically increased with the increase in pH from 2.0 to 3.0 and remained relatively constant at higher pHs up to 10.0. These results clearly show that the synthetic siderite adsorbed As(V) efficiently in a relatively wide pH range. It was reported that As(V) adsorption on the natural siderite was independent on pH between 4.0 and 9.0 [2]. Except for the batch at pH 2.0, equilibrium solutions had a neutral pH around 6.5 (data not shown). It means that the adsorbent had capability in maintaining a neutral solution pH and kept the adsorption system at near neutral pH during the experiments. This broad optimum pH could be explained by the amphoteric nature of Fe oxides/oxyhydroxides, since Fe hydroxide minerals mainly attributed to As(V) removal (which will be discussed later). The amphoteric nature of Fe oxides can be explained by Eqs. (9) and (10) [33,34].

$$\equiv FeOH^{2+} \Leftrightarrow \equiv FeOH + H^+ \quad (9)$$

$$\equiv FeOH \Leftrightarrow \equiv FeO^- + H^+ \quad (10)$$

In a low pH medium, the reaction Eqs. (9) and (10) shift towards left, resulting in an increase in the bulk solution pH. In a high pH medium, the acid dissociation dominates, which causes a decrease in the bulk solution pH [37].

In addition, the stable adsorption efficiency at pH 3.0–10.0 was expected to attribute to high dosage of the adsorbent with high adsorption capacity. In this case, although a proportion of the adsorbent was inactivated during the reaction with H^+ or OH^-, the residual was enough to adsorb the As from aqueous solution. The much low adsorption at pH 2.0 resulted from dissolution of the adsorbent, since quite high Fe concentration was found in aqueous solution (up to 270 mg/L).

It is believed that adsorption of As(V) species, such as $H_2AsO_4^-$ and $HAsO_4^{2-}$, onto Fe-containing substances takes place via Coulombic as well as Lewis acid–base interactions (ligand exchange reactions). In our study, slight dissolution of siderite would intro-

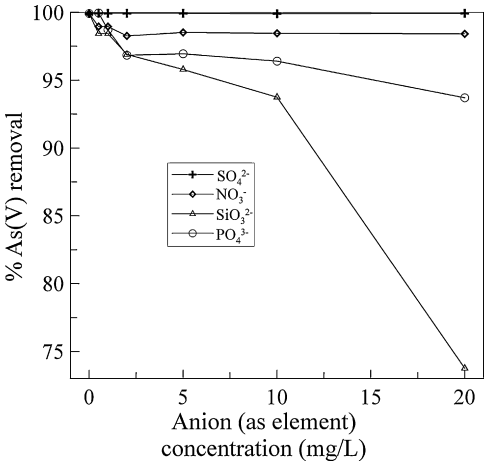

Fig. 6. Effect of presence of anions on As(V) adsorption (initial As(V) concentration = 1.0 mg/L, temperature = 25 °C, contact time = 3.0 h, adsorbent dosage = 2 g/L).

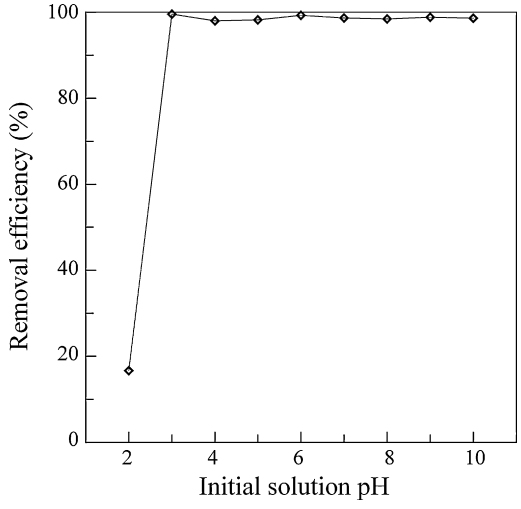

Fig. 5. Effect of solution pH on As(V) adsorption onto the synthetic siderite (initial As(V) concentration = 1.0 mg/L, temperature = 25 °C, contact time = 3.0 h, adsorbent dosage = 2 g/L).

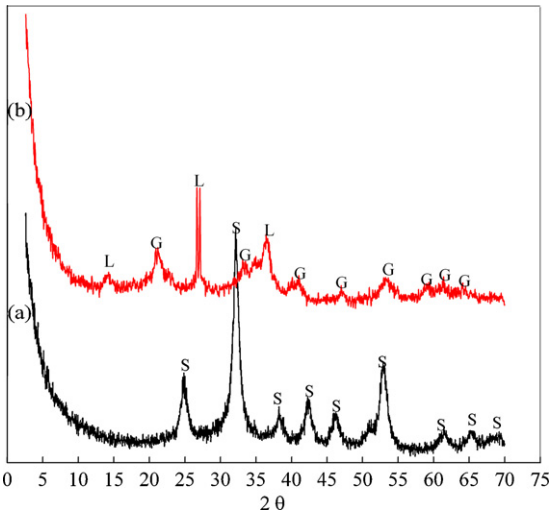

Fig. 7. XRD patterns of the pristine adsorbent (a) and the used adsorbent (b) (S, siderite; G, goethite; L, lepidocrocite).

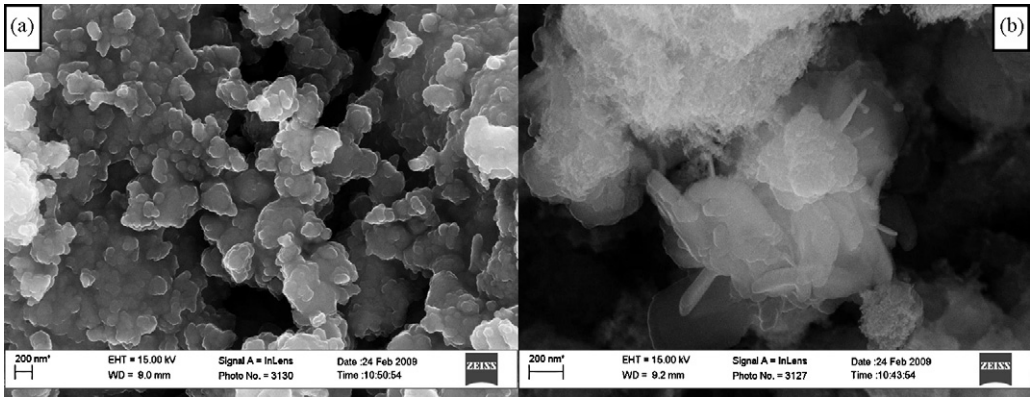

Fig. 8. SEM images of the pristine adsorbent (a) and the used adsorbent (b).

duce bicarbonate into solutions. Chemical processes, including bicarbonate buffering reactions and Eqs. (9) and (10), made solution pH approaching 6.5 when As(V) solution having initial pH 3.0–10.0 reacted with the synthetic siderite. Since the equilibrium pH tended to a constant around 6.5, Coulombic interaction remained relatively constant during batch experiments with initial pH 3.0–10.0. In addition, Lewis acid-base interactions would be independent on solution initial pH. However, As(V) adsorption was much greater at the higher adsorption rate at the lower pH on hydrous Fe oxide [35] and granular ferric hydroxide [8], in comparison with that at the higher pH.

3.6. Effect of competing anions on As removal

Arsenic(V) adsorption in the presence of competing anions (including NO_3^-, SO_4^{2-}, PO_4^{3-}, or SiO_3^{2-}) was investigated with 0.5, 1, 2, 5,10 and 20 mg/L of P (as PO_4^{3-}), N (as NO_3^-), S (as SO_4^{2-}), or Si (as SiO_3^{2-}) with an initial As(V) concentration of 1.0 mg/L at 25 °C. Results are shown in Fig. 6. The adverse effect of the anion on As(V) removal decreased in the following order: $SiO_3^{2-} > PO_4^{3-} > NO_3^- > SO_4^{2-}$. The removal of As(V) decreased significantly as PO_4^{3-} and SiO_3^{2-} concentrations increased in the separate solutions. When S (as SO_4^{2-}) concentration increased from 0.5 to 20 mg/L, the removal of As(V) by the synthetic siderite was not affected (Fig. 6). The SO_4^{2-} had no obvious effect on adsorption of As(V) because it did not compete with $HAsO_4^{2-}$. With the presence of 0.5 mg/L N as NO_3^-, removal efficiency reduced from 99.93% to 98.97% in comparison with the absence of NO_3^-. Above 2 mg/L N as NO_3^-, the effect levelled off.

As can be seen from Fig. 6, an increase in Si from 0.5 to 10 mg/L resulted in a decrease in removal efficiency from 98.44% to 93.75%, which amounts to a 5% decrease in As(V) adsorption. Above 10 mg/L Si, the adverse effect drastically increased. At 20 mg/L Si, the removal efficiency reduced to 73.76%. Meng et al. also found that As removal by Fe hydroxides was reduced from greater than 99% to approximately 85% when silicate concentration increased to approximately 0.7 mM [36]. In contrast, Zhang et al. observed a 30% decrease in As(V) adsorption when Si (as silicate) concentration increased from 1.4 to 5.0 mg/L [37]. Below 2.0 mg/L P as PO_4^{3-}, the change of As removal efficiency with PO_4^{3-} concentration is the same as SiO_3^{2-}. With an increase in P concentration from 0.5 to 2.0 mg/L, the As(V) removal efficiency steadily reduced from 99.93% to 96.85%. Above 2.0 mg/L, PO_4^{3-} had a less adverse impact on As(V) removal than SiO_3^{2-}. The evident reduce in As(V) removal in the presence of PO_4^{3-} and SiO_3^{2-} was believed to result from the competitive adsorption between As(V) and those anions for positively charged adsorption sites [36,38]. Guo et al. [2] also found that the presence of phosphate (10 mg/L in terms of P) reduced the uptake of As(V) by natural siderite from 54% to 28%. In Inner Mongolia, most high As groundwater had P concentrations ranging from <0.1 to 3.54 and Si concentrations from 3.5 to 16.9 mg/L [39,40]. It was speculated that the component adversely affecting As removal efficiency should be SiO_3^{2-} rather than PO_4^{3-} in case that the adsorbent is applied to remove As from high As groundwater in Inner Mongolia.

Effect of background electrolyte (NaCl) concentration was investigated with 0.001–0.1 mol/L NaCl as background electrolyte with an initial As(V) concentration of 1.0 mg/L at 25 °C. It was found that As(V) removal was not affected by the concentration of background electrolyte. Arsenic(V) removal efficiency was kept around 99.92% from As solution containing 0.001–0.1 mol/L NaCl (data not shown).

3.7. Mechanisms of As removal

It was found that siderite is the main mineralogical component in the synthesized material (Fig. 7a). After adsorption, most of siderite was changed into goethite and lepidocrocite (Fig. 7b). These freshly formed Fe-hydroxide minerals have a very high affinity for As [41,42]. The transformation of mineral phases during the adsorption was also manifested by the SEM images (Fig. 8). It can be noted that there were many spherical particles (~200 nm diameter) presented on the surface of the pristine adsorbent, whereas the used adsorbent was mainly covered by needle-like goethite and scaly lepidocrocite (~20 nm diameter). The goethite or ferrihydrite were loosely covered on the siderite matrix (Fig. 8b), which drastically enhanced the specific surface area. The transformation can take place as given in Eqs. (11) and (12).

$$FeCO_3 + H_2O \leftrightarrow Fe^{2+} + HCO_3^- + OH^- \quad (11)$$

$$2Fe^{2+} + \frac{1}{2}O_2 + H_2O \leftrightarrow 2FeOOH + 4H^+ \quad (12)$$

The same changes in mineralogical and structural characteristics were observed when the natural siderite was used to remove As from aqueous solution [13]. Therefore, mechanisms for As removal by the synthetic siderite were likely identical to those by the natural siderite. Chemical processes were the major factors controlling As adsorption characteristics, which is consistent with kinetic and thermodynamic study as stated above. The high adsorption capacity of the adsorbent possibly arose from both coprecipitation of the Fe hydroxides with As and subsequent adsorption of As on the fresh Fe hydroxides.

4. Conclusions

Arsenic(V) adsorption on the synthetic siderite significantly increased with an increase in contact time. The adsorption rate was

fast at the initial stage, followed by a slower rate, which well fitted a pseudo-second-order kinetics model. Temperature played an important role in the As adsorption kinetics. At higher temperature, As(V) exhibited greater removal rates. The adsorption closely followed Langmuir isotherm at low temperatures (i.e., 15 and 25 °C), while Freundlich isotherm at relatively higher temperatures (35–45 °C). Thermodynamic study shows that As(V) adsorption onto the synthetic siderite was an endothermic process, indicating As(V) adsorption capacity increased with an increase in reaction temperature. The adsorption was spontaneous and favorable at the temperature investigated. Arsenic(V) removal was independent on the initial pH between 3.0 and 10.0. The presence of SO_4^{2-} and NO_3^- had no significant effect on the uptake of As(V) by the adsorbent, while PO_4^{3-} and SiO_3^{2-} impeded As(V) adsorption. The adverse effect on As adsorption was enhanced as PO_4^{3-} or SiO_3^{2-} concentration increased. Chemical processes were the major factors controlling As adsorption characteristics. The high removal capacity of the adsorbent may result from both coprecipitation of As with the Fe hydroxides (i.e., goethite and lepidocrocite) forming during the reaction and subsequent adsorption of As on these fresh Fe hydroxide minerals. The study results presented here have confirmed the potential of synthetic siderite as an efficient material for the treatment of As(V). Although we have presented evidence that As(V) can be removed by adsorption/precipitation on synthetic siderite in a relatively short time in static conditions, the synthetic siderite could be used as a coating material on grained particles (such as quartz sand and feldspar) and/or an active agent in aggregated adsorbents for the purpose of fixed bed application.

Acknowledgements

Funding for this research has been provided by the National Natural Science Foundation of China (Nos. 40572145 and 40872160), the Program for New Century Excellent Talents in University (No. NCET-07-0770), the Cultivation Fund of the Key Scientific and Technical Innovation Project, Ministry of Education of China (No. 708012), and the National Key-technologies R&D Program (No. 2006BAJ08B04) of the 11th 5-year Plan of the People's Republic of China. The authors would like to thank Mr. Chao Wei and Ms. Bo Zhang for laboratory assistances.

References

[1] P.L. Smedley, D.G. Kinniburgh, A review of the source, behaviour and distribution of arsenic in natural waters, Appl. Geochem. 17 (2002) 517–568.
[2] H.M. Guo, D. Stüben, Z. Berner, Removal of arsenic from aqueous solution by natural siderite and hematite, Appl. Geochem. 22 (2007) 1039–1051.
[3] W.E. Morton, D.A. Dunette, Health effect of environmental arsenic, in: J.O. Nriagu (Ed.), Arsenic in the Environment, Part II: Human and Ecosystem Effects, Wiley and Sons, New York, 1994, pp. 17–34.
[4] World Health Organization, Guidelines for Drinking-Water Quality, Health Criteria and other Supporting Information, second ed., vol. 2, WHO, Geneva, Switzerland, 1996, pp. 940–949.
[5] European Commission, Directive related with drinking water quality intended for human consumption, Brussels, Belgium, 98/83/EC, 1998.
[6] EPA Office of Groundwater and Drinking Water, Implementation guidance for the arsenic rule, EPA Report-816-D-02-005, Cincinnati, USA, 2002.
[7] P. Lakshmipathiraj, B.R.V. Narasimhan, S. Prabhakar, R.G. Bhaskar, Adsorption studies of arsenic on Mn-substituted iron oxyhydroxide, J. Colloid Interf. Sci. 304 (2006) 317–322.
[8] K. Banerjee, G.L. Amy, M. Prevost, S. Nour, M. Jekel, P.M. Gallagher, C.D. Blumenschein, Kinetic and thermodynamic aspects of adsorption of arsenic onto granular ferric hydroxide (GFH), Water Res. 42 (2008) 3371–3378.
[9] S. Jessen, F. Larsen, C.B. Koch, E. Avin, Sorption and desorption of arsenic to ferrihydrite in a sand filter, Environ. Sci. Technol. 39 (2005) 8045–8051.
[10] X. Sun, H.E. Doner, Adsorption and oxidation of arsenite on goethite, Soil Sci. 163 (1998) 278–287.
[11] N.P. Nikolaidis, G.M. Dobbs, J.A. Lackovic, Arsenic removal by zerovalent iron: field, laboratory and modeling studies, Water Res. 37 (2003) 1417–1425.
[12] Y. Zhang, M. Yang, X. Huang, Arsenic(V) removal with a Ce(IV)-doped iron oxide adsorbent, Chemosphere 51 (2003) 945–952.
[13] H.M. Guo, D. Stüben, Z. Berner, Adsorption of arsenic(III) and arsenic(V) from groundwater using natural siderite as the adsorbent, J. Colloid Interf. Sci. 315 (2007) 47–53.
[14] C. Su, R.W. Puls, Arsenate and arsenite removal by zero-valent iron: kinetics, redox transformation, and implications for in situ groundwater remediation, Environ. Sci. Technol. 35 (2001) 1487–1492.
[15] S. Goldberg, Competitive adsorption of arsenate and arsenite on oxides and clay minerals, Soil Sci. Soc. Am. J. 66 (2002) 413–421.
[16] K. Tyrovola, N.P. Nikolaidis, N. Veranis, N. Kallithrakas-Kontos, P.E. Koulouridakis, Arsenic removal from geothermal waters with zero-valent iron—effect of temperature, phosphate and nitrate, Water Res. 40 (2006) 2375–2386.
[17] H. Genç-Fuhrman, J.C. Tjell, D. Mcconchie, Adsorption of arsenic from water using activated neutralized red mud, Environ. Sci. Technol. 38 (2004) 2428–2434.
[18] T.S. Singh, K.K. Pant, Equilibrium, kinetics and thermodynamic studies for adsorption of As(III) on activated alumina, Sep. Purif. Technol. 36 (2004) 139–147.
[19] I.A. Oke1, N.O. Olarinoye, S.R.A. Adewusi, Adsorption kinetics for arsenic removal from aqueous solutions by untreated powdered eggshell, Adsorption 14 (2007) 73–83.
[20] Y.S. Ho, A.E. Ofomaja, Pseudo-second-order model for lead ion sorption from aqueous solutions onto palm kernel fiber, J. Hazard. Mater. B129 (2006) 137–142.
[21] Y.S. Ho, G. McKay, A kinetic study of dye sorption by biosorbent waste product pith, Resour. Conserv. Recy. 25 (1999) 171–193.
[22] W.J. Weber Jr., J.C. Morris, Kinetics of adsorption on carbon from solution, J. Sanit. Eng. Div., Proc. Am. Soc. Civil Eng. 89 (1963) 31–42.
[23] M. Badruzzaman, P. Westerhoff, D.R.U. Knappe, Intraparticle diffusion and adsorption of arsenate onto granular ferric hydroxide (GFH), Water Res. 38 (2004) 4002–4012.
[24] Y. Kim, C. Kim, I. Choi, S. Rengaraj, J. Yi, Arsenic removal using mesoporous alumina prepared via a templating method, Environ. Sci. Technol. 38 (2004) 924–931.
[25] H.M. Guo, D. Stüben, Z. Berner, Q.C. Yu, Characteristics of arsenic adsorption from aqueous solution: effect of arsenic species and natural adsorbents, Appl. Geochem. 24 (2009) 657–663.
[26] C. Namasivayam, S. Senthilkumar, Removal of arsenic(V) from aqueous solution using industrial solid waste: adsorption rates and equilibrium studies, Ind. Eng. Chem. Res. 37 (1998) 4816–4822.
[27] O.S. Thirunavukkarasu, T. Viraraghavan, K.S. Subramanian, Arsenic removal from drinking water using Fe oxide-coated sand, Water Air Soil Pollut. 142 (2003) 95–111.
[28] S. Bang, M. Patel, L. Lippincott, X. Meng, Removal of arsenic from groundwater by granular titanium dioxide adsorbent, Chemosphere 60 (2005) 389–397.
[29] P. Lakshmipathiraj, B.R.V. Narasimhan, S. Prabhakar, G. Bhaskar Raju, Adsorption of arsenate on synthetic goethite from aqueous solutions, J. Hazard. Mater. B136 (2006) 281–287.
[30] Y.Y. Chang, K.H. Song, J.K. Yang, Removal of As(III) in a column reactor packed with iron-coated sand and manganese-coated sand, J. Hazard. Mater. 150 (2008) 565–572.
[31] K.K. Panday, G. Prasad, V.N. Singh, Copper (II) removal from aqueous solution by fly ash, Water Res. 19 (1985) 869–876.
[32] H.S. Altundoğan, S. Altundoğan, F. Tümen, M. Bildik, Arsenic removal from aqueous solutions by adsorption on red mud, Waste Manage. 20 (2000) 761–767.
[33] S.M. Ahmed, Studies of the dissociation of oxide surface at the liquid–solid interface, Can. J. Chem. 44 (1966) 1663–1670.
[34] R.M. Cornell, U. Schwertmann, The Fe Oxides-Structure, Properties, Reactions, Occurrence and Uses, VCH Verlagsgesellschaft, VCH Publishers, New York, 1996.
[35] K.P. Raven, A. Jain, R.H. Loeppert, Arsenite and arsenate adsorption on ferrihydrite: kinetics, equilibrium, and adsorption envelope, Environ. Sci. Technol. 32 (1998) 344–349.
[36] X.G. Meng, G.P. Korfiatis, S. Bang, K.W. Bang, Combined effects of anions on arsenic removal by iron hydroxides, Toxicol. Lett. 133 (2002) 103–111.
[37] W. Zhang, P. Singh, E. Paling, S. Delides, Arsenic removal from contaminated water by natural iron ores, Miner. Eng. 17 (2004) 517–524.
[38] C. Su, R.W. Puls, Arsenate and arsenite removal by zerovalent Fe: effects of phosphate, silicate, carbonate, borate, sulfate, chromate, molybdate, and nitrate, relative to chloride, Environ. Sci. Technol. 35 (2001) 4562–4568.
[39] H.M. Guo, S.Z. Yang, X.H. Tang, Y. Li, Z.L. Shen, Groundwater geochemistry and its implications for arsenic mobilization in shallow aquifers of the Hetao Basin, Inner Mongolia, Sci. Total Environ. 393 (2008) 131–144.
[40] P.L. Smedley, M. Zhang, G. Zhang, Z. Luo, Mobilisation of arsenic and other trace elements in fluviolacustrine aquifers of the Huhhot Basin, Inner Mongolia, Appl. Geochem. 18 (2003) 1453–1477.
[41] J.A. Munoz, A. Gonzalo, M. Valiente, Arsenic adsorption by Fe(III)-loaded open-celled cellulose sponge: thermodynamic and selectivity aspects, Environ. Sci. Technol. 36 (2002) 3405–3411.
[42] Z.M. Gu, J. Fang, B.L. Deng, Preparation and evaluation of GAC-based Fe-containing adsorbents for arsenic removal, Environ. Sci. Technol. 39 (2005) 3833–3843.